Electronic Supplementary Material (ESI) for Inorganic Chemistry Frontiers.

CuS-Ni_3S_2 in-situ grown from three-dimensional porous bimetallic foam for efficient oxygen evolution

Nan Zhang, Ying Gao, Yahui Mei, Jian Liu, Weiyu Song*, Ying Yu**

State Key Laboratory of Heavy Oil Processing, College of Science, China University of Petroleum, Beijing, 102249, China

*Corresponding authors:

*E-mail: zhangnan@cup.edu.cn (Nan Zhang)

*E-mail: songwy@cup.edu.cn (Weiyu Song)

*E-mail: yuying@cup.edu.cn (Ying Yu)

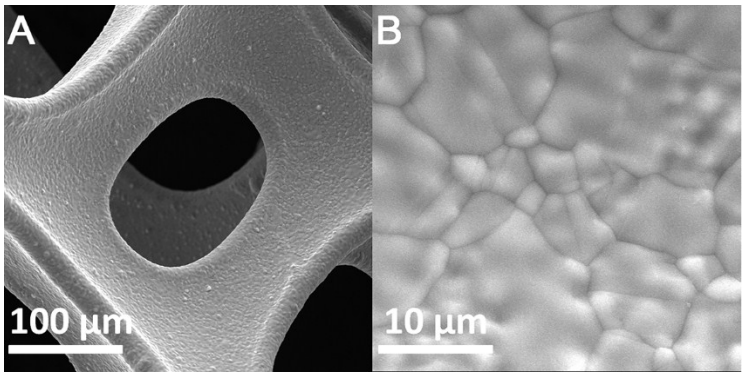

Fig. S1 (A-B) SEM images at different magnifications of bare NF.

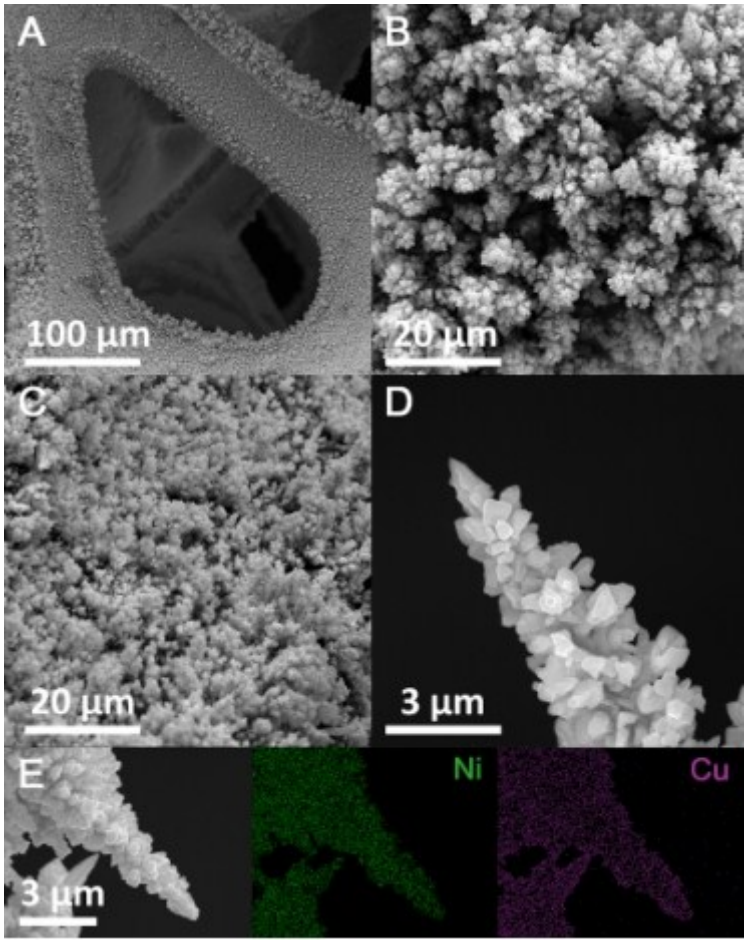

Fig. S2 (A-C) SEM images at different magnifications of the electrodeposited CuNi/NF substrate with high porosity, (D) SEM image and (E) EDX mapping images of the CuNi alloy nanodentrite.

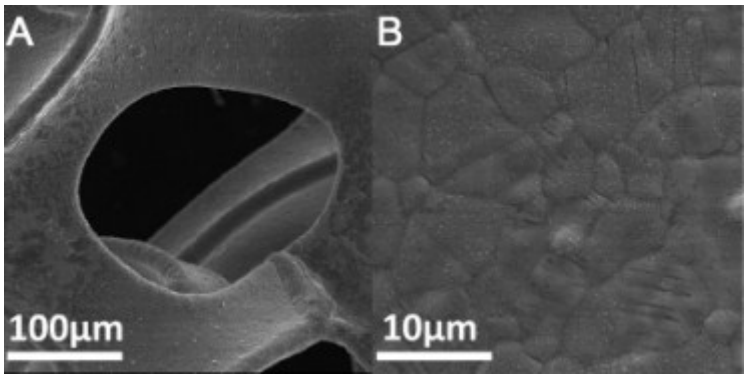

Fig. S3 SEM images of electrodeposited Ni/NF at different magnifications.

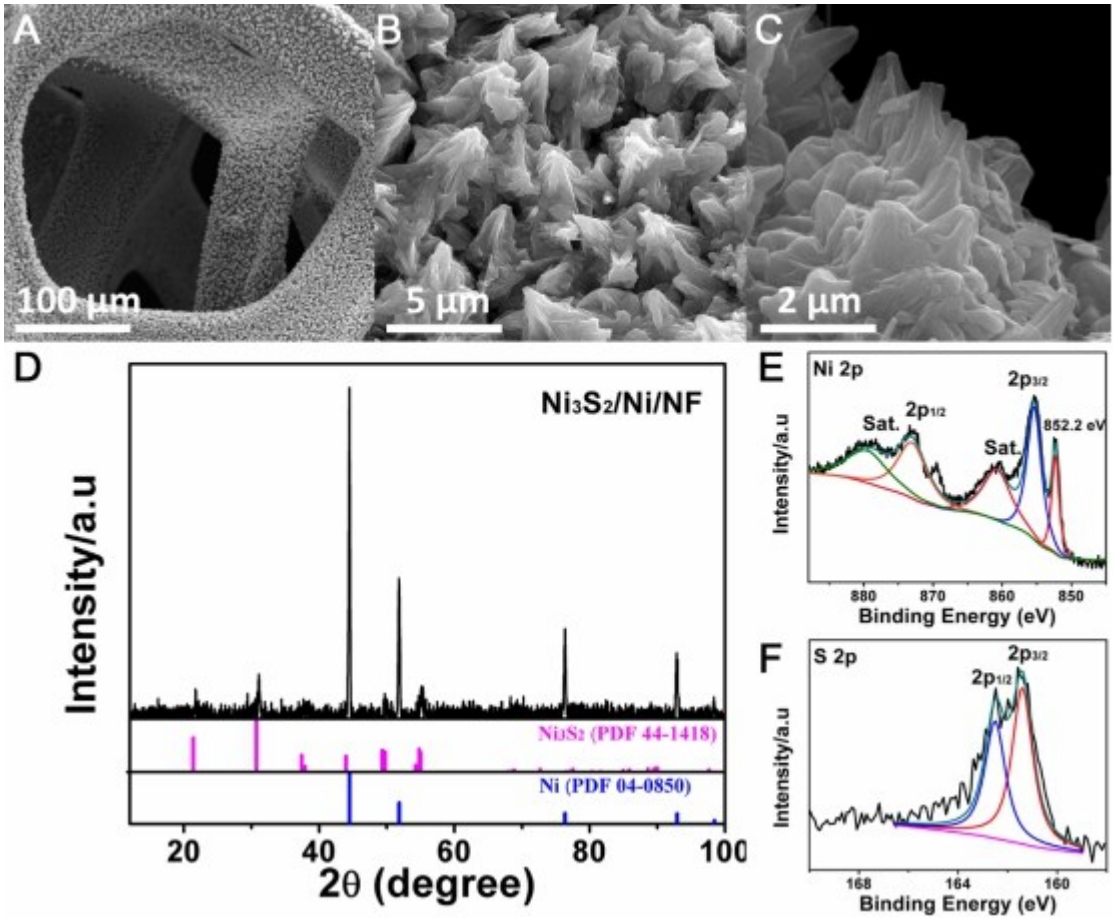

Fig. S4 (A-C) SEM images and (D) XRD patterns of Ni_3S_2/Ni/NF. XPS spectra in (E) Ni 2p and (F) S 2p regions of Ni_3S_2/Ni/NF. Compared with CuS-Ni_3S_2/CuNi/NF, Ni region shows an additional peak at 852.2 eV, belonging to Ni_3S_2 as reported.[1, 2]

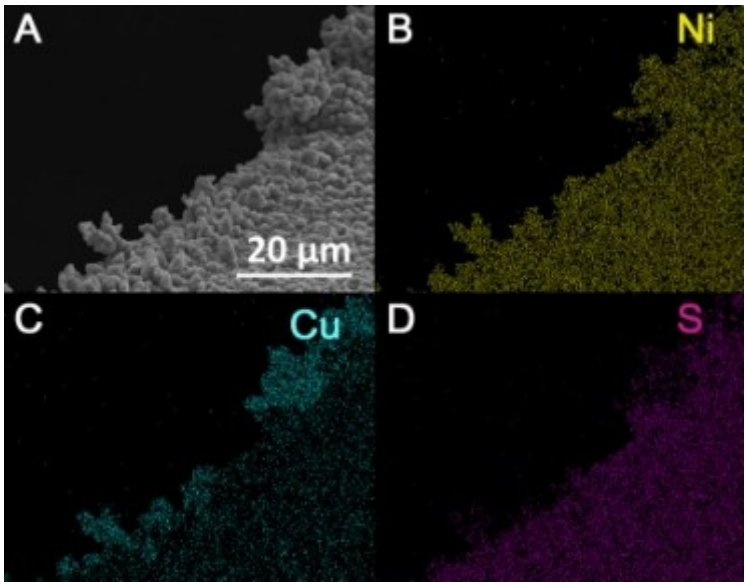

Fig. S5 EDX mapping images of CuS-Ni_3S_2/CuNi/NF electrode skeleton.

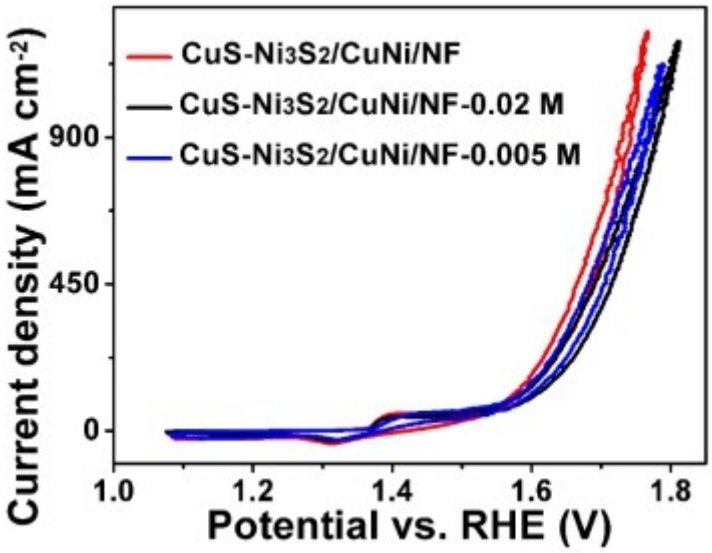

Fig. S6 CV curves of different catalytic electrodes synthesized by employing the different concentration of thiourea.

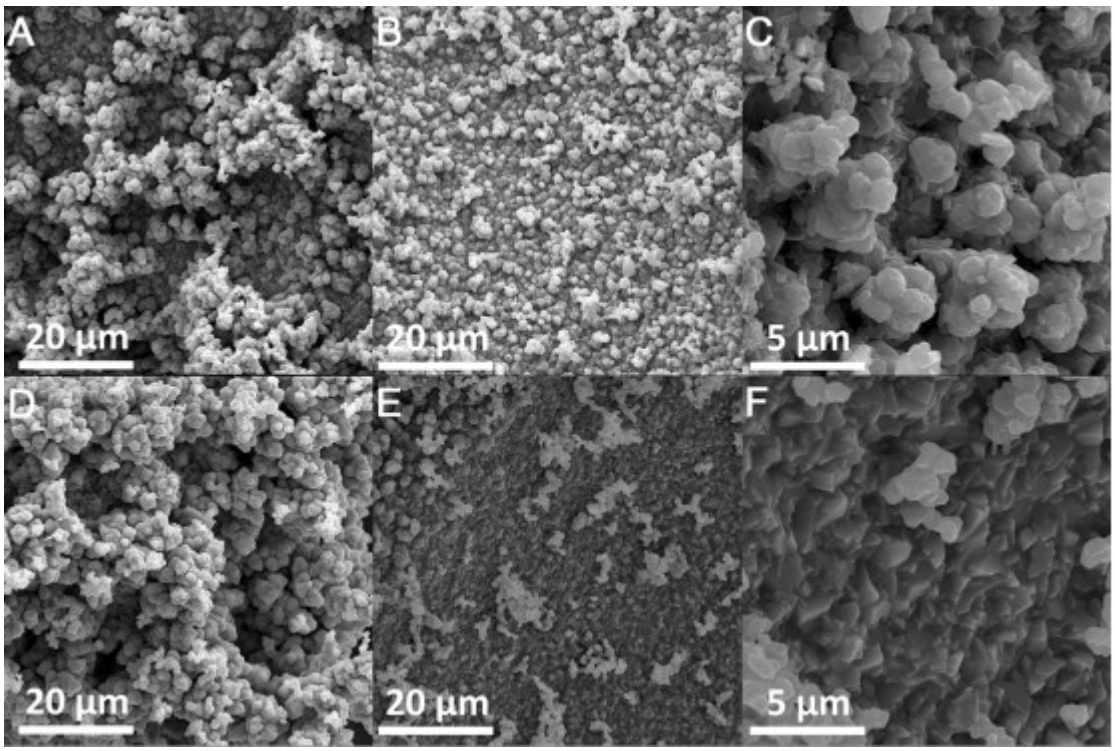

Fig. S7 SEM images of (A-C) CuS-Ni_3S_2/CuNi/NF-0.02 M and (D-F) CuS-Ni_3S_2/CuNi/NF-0.005 M.

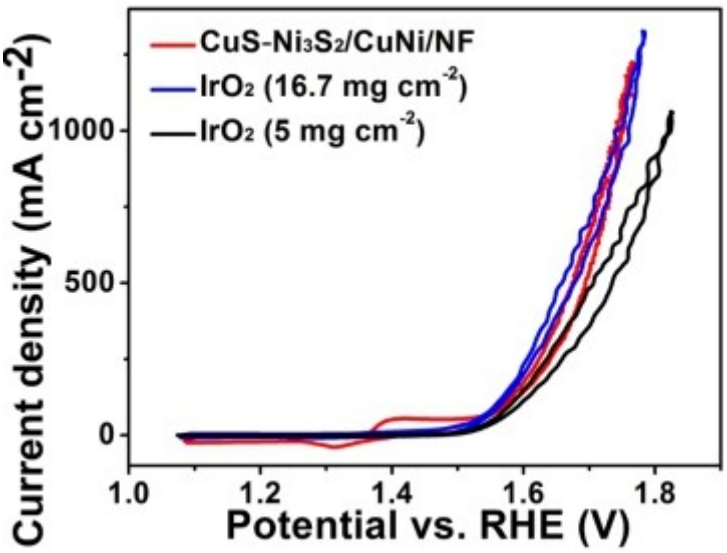

Fig. S8 CV curves of CuS-Ni_3S_2/CuNi/NF and IrO_2 decorated NF (abbreviated to IrO_2) with the same loading mass (16.7 mg cm^{-2}), and IrO_2 with the loading mass of 5 mg cm^{-2}.

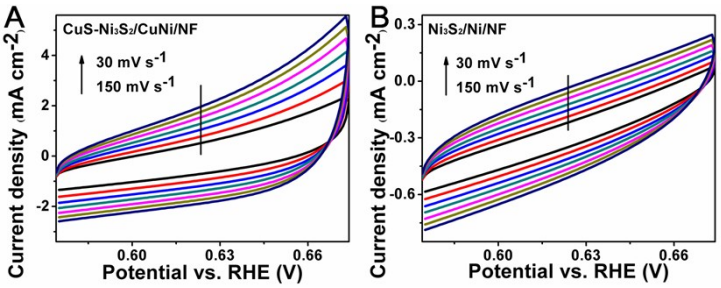

Fig. S9 CV curves measured in non-faradaic potential from 0.574 V to 0.674 V at different scan rates: 30, 50, 70, 90, 110, 130 and 150 mV s^{-1} for (A) CuS-Ni_3S_2/CuNi/NF and (B) Ni_3S_2/Ni/NF electrodes.

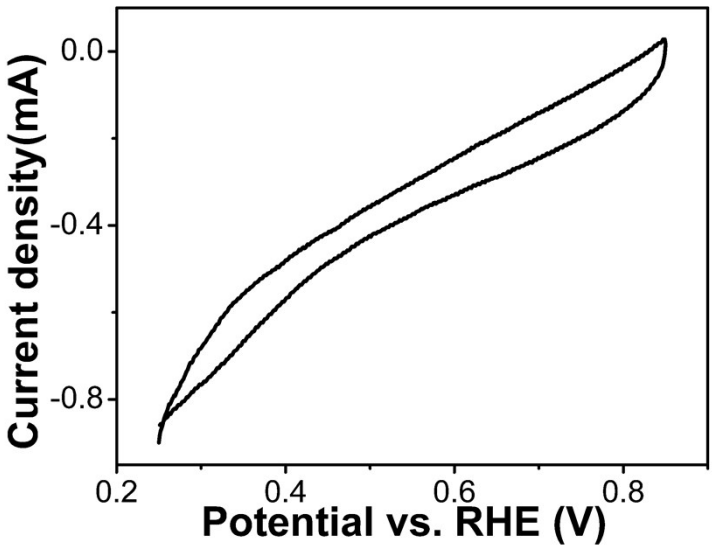

Fig. S10 CV curve of CuS-Ni_3S_2/CuNi/NF in 1 M phosphate buffered saline (PBS) solution (pH = 7.0) at a scan rate of 50 mV s^{-1}.

Calculation of active sites:

CV measurements were measured at 50 mV s^{-1} in 1 M solution PBS (pH = 7.0). Later, the absolute components of the voltammetric charges (cathodic and anodic) reported during one single blank measurement were added. Assuming a one electron redox process, this absolute charge was divided by two. The value was then divided by the Faraday constant to get the number of active sites (N) of catalysts.

$$\mathbf{N = \frac{Q}{2F} = \frac{\int IV / \upsilon}{2F}}$$

Q: the CV charge capacity obtained by integrating the CV curves.
F: Faraday constant (96485 C/mol).
I: current density (A)
V: voltage (V)
υ : scan rate (V s^{-1})

TOF calculation:

When the number of active sites is known, the turnover frequencies (s^{-1}) were calculated via the following equation:

$$\mathbf{TOF = \frac{I}{FN}\frac{1}{4}}$$

I: Current (A) during the LSV measurement in 1.0 M KOH.
F: Faraday constant (96485 C/mol).
N: Number of active sites (mol).
The factor 1/4 arrives by taking into account that four electrons are required to form one oxygen molecule.

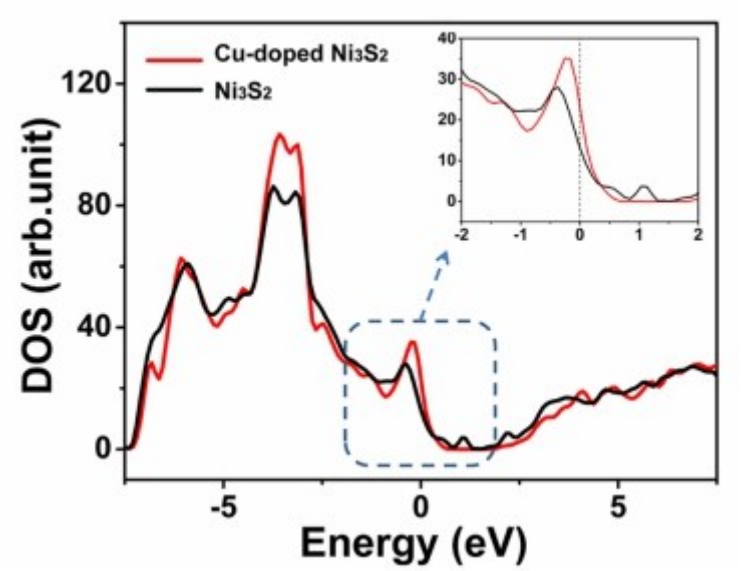

Fig. S11 Calculated density of states (DOS) for CuS-Ni_3S_2 and pristine Ni_3S_2. The Fermi level is set at 0 eV.

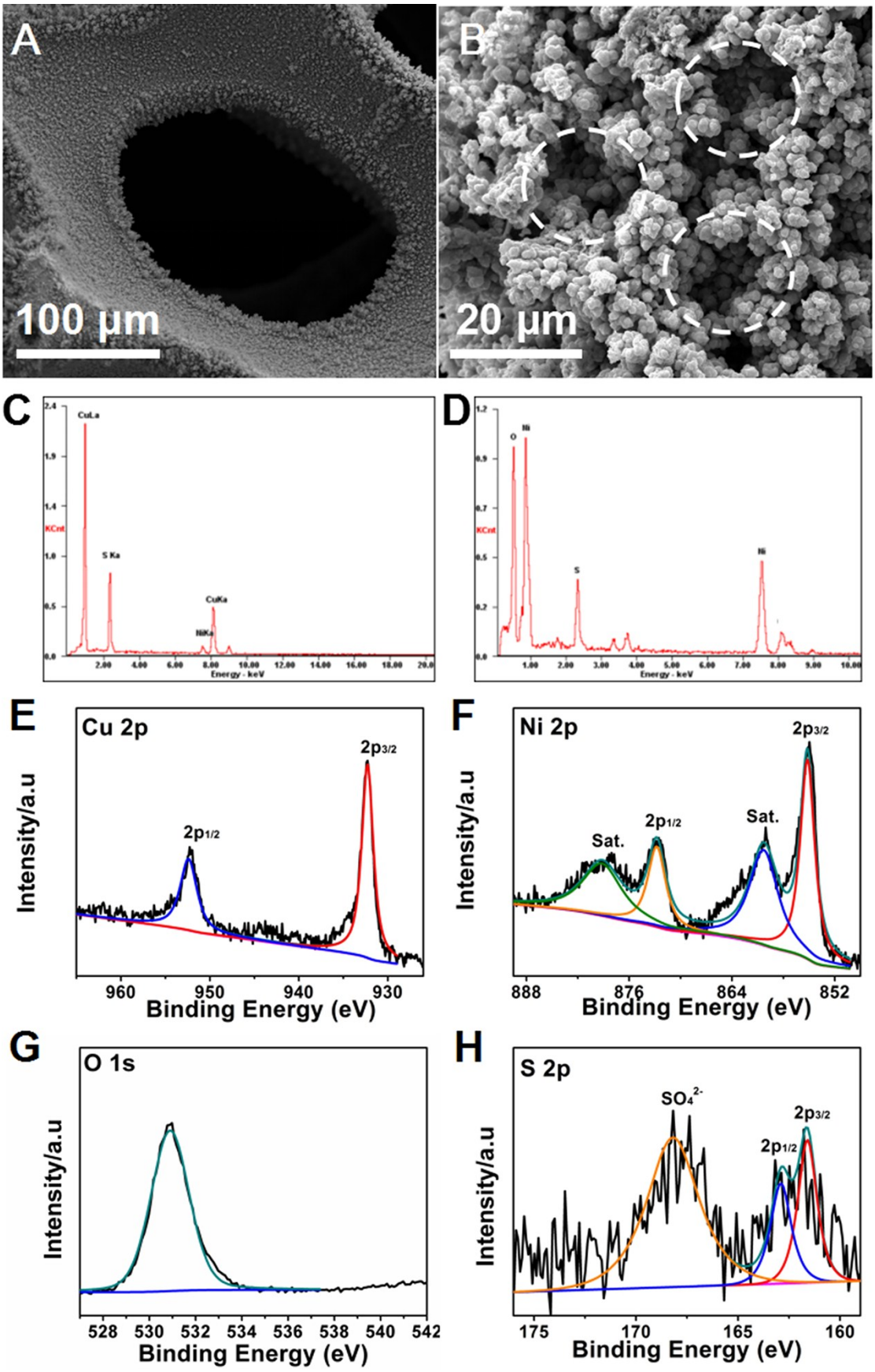

Fig. S12 (A-B) SEM at different magnifications, EDX spectra of CuS-Ni_3S_2/CuNi/NF (C) before and (D) after the OER durability test at 100 mA cm^{-2} for 15 h and XPS

spectra in (E) Cu, (F) Ni, (G) O and (H) S regions of CuS-Ni_3S_2/CuNi/NF after the OER durability test at 100 mA cm^{-2} for 15 h.

No O peak could be observed in the EDX spectrum of CuS-Ni_3S_2/CuNi/NF before the 15 h durability test (Fig. S12C), while a strong O peak appeared after the 15 h durability test (Fig. S12D), indicating that CuS-Ni_3S_2/CuNi/NF was oxidized after the vigorous and long OER process. Furthermore, XPS spectra were utilized to further investigate the surface chemical composition after the 15 h duration test. In Fig. S12F, it is found that the spin–orbit splitting energy between the two Ni 2p peaks is about 17.6 eV, indicating the formation of $Ni(OH)_2$.[3] The O 1s spectrum in Fig. S12G shows a peak at 531.02 eV which can be attributed to the O atoms in OH^-,[4] further demonstrating the formation of $Ni(OH)_2$ after OER durability test. Therefore, Ni_3S_2 in CuS-Ni_3S_2/CuNi/NF was oxidized to $Ni(OH)_2$ during OER process.

Table S1. CuNi/NF with several Ni-based and Cu-based OER catalysts reported recently.

Catalyst	Electrolyte	Current ($mA\ cm^{-2}$)	Overpotential (η, mV)	Reference
CuS-Ni_3S_2/CuNi/NF	1.0 M KOH	100 200 500 1000	337 379 444 509	this work
Ni_3S_2/Au/Si	1.0 M KOH	10	400	[5]
CdS/Ni_3S_2/PNF[I]	1.0 M KOH	10 100	110 ~530	[6]
MoO_x/Ni_3S_2/NF	1.0 M KOH	10 100 200 500	136 310 ~360 ~520	[7]
NF-Ni_3S_2/NF	1.0 M KOH	20 100 200	230 ~340 ~410	[8]
$Ni_xCo_{3-x}S_4$/Ni_3S_2/NF	1.0 M KOH	10 100	300 570	[9]
Ni_3S_2@G@Co_9S_8	1.0 M KOH	10 100	210 ~350	[10]
Co_3O_4@Ni_3S_2/NF	1.0 M KOH	20 100	260 ~500	[1]
NiCoS/$Ti_3C_2T_x$	1.0 M KOH	10	365	[11]
NiCoP **NiMnP** **NiMoP**	1.0 M KOH	20 20 20	410 450 430	[12]
Ni/Ni_3C	0.1 M KOH	10	350	[13]
$Ni_{11}(HPO_3)_8(OH)_6$/NF	1.0 M KOH	10 100	232 362	[14]
$Ni(OH)_2$/Ni_3S_2	1.0 M KOH	20 100	270 400	[15]
CuO@Ni–PNA/CF[II]	1.0 M KOH	30 100 200	275 ~360 ~380	[16]
Co-CuO NA/CF[III]	1.0 M KOH	50 100	299 330	[17]

I: PNF: plasma-treated nickel foam
II, III: CF: copper foam

Reference

1. Y. Gong, Z. Xu, H. Pan, Y. Lin, Z. Yang and X. Du, *J. Mater. Chem. A*, 2018, **6**, 5098-5106.
2. Y. Yang, K. Zhang, H. Lin, X. Li, H. C. Chan, L. Yang and Q. Gao, *ACS Catal.*, 2017, **7**, 2357-2366.
3. D. Merki, S. Fierro, H. Vrubel and X. Hu, *Chem. Sci.*, 2011, **2**, 1262-1267.
4. H. Ashassi-Sorkhabi and P. La'le Badakhshan, *Appl. Surf. Sci.*, 2017, **419**, 165-176.
5. T. A. Ho, C. Bae, H. Nam, E. Kim, S. Y. Lee, J. H. Park and H. Shin, *ACS Appl. Mater. Interfaces*, 2018, **10**, 12807-12815.
6. S. Qu, J. Huang, J. Yu, G. Chen, W. Hu, M. Yin, R. Zhang, S. Chu and C. Li, *ACS Appl. Mater. Interfaces*, 2017, **9**, 29660-29668.
7. Y. Wu, G.-D. Li, Y. Liu, L. Yang, X. Lian, T. Asefa and X. Zou, *Adv. Func. Mater*, 2016, **26**, 4839-4847.
8. L. Zeng, K. Sun, Z. Yang, S. Xie, Y. Chen, Z. Liu, Y. Liu, J. Zhao, Y. Liu and C. Liu, *J. Mater. Chem. A*, 2018, **6**, 4485-4493.
9. Y. Y. Wu, Y. P. Liu, G. D. Li, X. Zou, X. R. Lian, D. J. Wang, L. Sun, T. Asefa and X. X. Zou, *Nano Energy*, 2017, **35**, 161-170.
10. Q. C. Dong, Y. Z. Zhang, Z. Y. Dai, P. Wang, M. Zhao, J. J. Shao, W. Huang and X. C. Dong, *Nano Res.*, 2018, **11**, 1389-1398.
11. H. Zou, B. He, P. Kuang, J. Yu and K. Fan, *ACS Appl. Mater. Interfaces*, 2018, **10**, 22311-22319.
12. H.-W. Man, C.-S. Tsang, M. M.-J. Li, J. Mo, B. Huang, L. Y. S. Lee, Y.-C. Leung, K.-Y. Wong and S. C. E. Tsang, *Chem. Commun.(Cambridge, England)*, 2018.
13. Q. Qin, J. Hao and W. Zheng, *ACS Appl. Mater. Interfaces*, 2018, **10**, 17827-17834.
14. P. W. Menezes, C. Panda, S. Loos, F. Bunschei-Bruns, C. Walter, M. Schwarze, X. Deng, H. Dau and M. Driess, *Energy Environ. Sci.*, 2018, **11**, 1287-1298.
15. X. Du, Z. Yang, Y. Li, Y. Gong and M. Zhao, *J. Mater. Chem. A*, 2018, **6**, 6938-6946.
16. B. Chang, S. Hao, Z. X. Ye and Y. C. Yang, *Chem. Commun.,* 2018, **54**, 2393-2396.
17. X. L. Xiong, C. You, Z. Liu, A. M. Asiri and X. P. Sun, *ACS Sustain. Chem. Eng.*, 2018, **6**, 2883-2887.